bioRxiv preprint doi: https://doi.org/10.1101/695007; this version posted November 1, 2019. The copyright holder for this preprint (which was not certified by peer review) is the author/funder. All rights reserved. No reuse allowed without permission.

Novel insights into the taxonomic diversity and molecular mechanisms of bacterial Mn(III) reduction

Nadia Szeinbaum[1,2,5*], Brook L. Nunn[3], Amanda R. Cavazos[2], Sean A. Crowe[3], Frank J. Stewart[1], Thomas J. DiChristina[1], Christopher T. Reinhard[2,5], and Jennifer B. Glass[2,5]*

[1]School of Biological Sciences, Georgia Institute of Technology, Atlanta, GA, USA

[2]School of Earth and Atmospheric Sciences, Georgia Institute of Technology, Atlanta, GA, USA

[3]Department of Genome Sciences, University of Washington, Seattle, WA, USA

[4]Department of Microbiology & Immunology and Department of Earth, Ocean, & Atmospheric Sciences, University of British Columbia, Vancouver, Canada

[5]NASA Astrobiology Institute, Alternative Earths Team, Mountain View, CA

*Corresponding author: jennifer.glass@eas.gatech.edu

Running title: Novel undecaheme in Betaproteobacteria

bioRxiv preprint doi: https://doi.org/10.1101/695007; this version posted November 1, 2019. The copyright holder for this preprint (which was not certified by peer review) is the author/funder. All rights reserved. No reuse allowed without permission.

Originality-significance Statement: The prevalence of Mn(III)-ligand complexes in diverse aquatic environments is a recent geochemical discovery. Thus far, microbially-driven Mn(III) reduction has only been associated with *Gammaproteobacteria* encoding three-component outer-membrane porin-cytochrome c conduits. Here, we demonstrate that *Betaproteobacteria* dominate in abundance and protein expression during Mn(III) reduction in an enrichment culture. Using metaproteomics, we detect for the first time that *Betaproteobacteria* express a two-component porin-cytochrome c conduit, and an uncharacterized extracellular undecaheme c-type cytochrome. Although undecahemes have never been reported in *Betaproteobacteria*, we find that they are widespread in uncultivated strains. These results widen the phylogenetic diversity of Mn(III)-reducing bacteria, and provide new insights into potential molecular mechanisms for soluble Mn(III) reduction.

bioRxiv preprint doi: https://doi.org/10.1101/695007; this version posted November 1, 2019. The copyright holder for this preprint (which was not certified by peer review) is the author/funder. All rights reserved. No reuse allowed without permission.

Summary: Soluble ligand-bound Mn(III) can support anaerobic microbial respiration in diverse aquatic environments. Thus far, Mn(III) reduction has only been associated with certain *Gammaproteobacteria*. Here, we characterized microbial communities enriched from Mn-replete sediments of Lake Matano, Indonesia. Our results provide the first evidence for biological reduction of soluble Mn(III) outside *Gammaproteobacteria*. Metagenome assembly and binning revealed a novel betaproteobacterium, which we designate "*Candidatus* Dechloromonas occultata." This organism dominated the enrichment and expressed a porin-cytochrome c complex typically associated with iron-oxidizing *Betaproteobacteria* and a novel cytochrome c-rich protein cluster (Occ), including an undecaheme putatively involved in extracellular electron transfer. The *occ* gene cluster was detected in diverse aquatic bacteria, including uncultivated *Betaproteobacteria* from the deep subsurface. These observations provide new insight into the taxonomic and functional diversity of microbially-driven Mn(III) reduction in natural environments.

bioRxiv preprint doi: https://doi.org/10.1101/695007; this version posted November 1, 2019. The copyright holder for this preprint (which was not certified by peer review) is the author/funder. All rights reserved. No reuse allowed without permission.

Introduction. Manganese(III) is a strong oxidant with a reduction potential close to molecular oxygen (Kostka et al., 1995). Ligand-bound Mn(III) is often the most abundant dissolved Mn species in sediment porewaters (Madison et al., 2013; Oldham et al., 2019) and soils (Heintze and Mann, 1947). In the deep subsurface, microbes may rely on simple electron and carbon sources such as CH_4, and metal oxide electron acceptors like Mn(III), to fuel anaerobic respiration (Beal et al., 2009). Manganese reduction coupled to CH_4 oxidation is a thermodynamically favorable metabolism, and its natural occurrence is supported by biological and geochemical evidence (Crowe et al., 2011; Riedinger et al., 2014). Despite clear evidence for the environmental importance of Mn(III), knowledge about microbial Mn(III) cycling pathways remain fragmentary.

To date, only *Shewanella* spp. (*Gammaproteobacteria*) have been confirmed to respire soluble Mn(III) (Kostka et al., 1995; Szeinbaum et al., 2014). *Shewanella* respire Mn(III) using the Mtr pathway (Szeinbaum et al., 2017), a porin-cytochrome (PCC) conduit that transports electrons across the periplasm for extracellular respiration of Mn(III/IV), Fe(III), and other metals (Richardson et al., 2012; Shi et al., 2016). Many Fe(II)-oxidizing *Betaproteobacteria* also contain PCCs (MtoAB, generally lacking the C subunit), which are proposed to oxidize Fe(II) to Fe(III) by running the PCC in reverse (Emerson et al., 2013; Kato et al., 2015; He et al., 2017). In some metal-reducing *Gammaproteobacteria* and *Deltaproteobacteria*, extracellular undecaheme (11-heme) UndA is thought to play a key functional role in soluble Fe(III) reduction (Fredrickson et al., 2008; Shi et al., 2011; Smith et al., 2013; Yang et al., 2013). UndA's crystal structure shows a surface-exposed heme surrounded by positive charges, which may bind negatively-charged soluble iron chelates (Edwards et al., 2012).

bioRxiv preprint doi: https://doi.org/10.1101/695007; this version posted November 1, 2019. The copyright holder for this preprint (which was not certified by peer review) is the author/funder. All rights reserved. No reuse allowed without permission.

Environmental omics suggests that metal reduction by *Betaproteobacteria* may be widespread in the deep subsurface (Anantharaman et al., 2016; Hernsdorf et al., 2017). However, only a few Fe(III)-reducing *Betaproteobacteria* isolates have been characterized (Cummings et al., 1999; Finneran et al., 2003), and little is known about metal reduction pathways in *Betaproteobacteria*. Here, we explored microbial Mn(III) reduction in enrichments inoculated with sediment from Lake Matano, Indonesia, which has active microbial Mn and methane (CH_4) cycles (Jones et al., 2011). Our results provide the first evidence for biological reduction of soluble Mn(III) outside *Gammaproteobacteria*.

Results and discussion

Enrichment of Mn(III)-reducing populations. We designed an enrichment strategy to select for microbes capable of anaerobic CH_4 oxidation coupled to soluble Mn(III) reduction by incubating anoxic Lake Matano communities with soluble Mn(III)-pyrophosphate as the electron acceptor (with 2% O_2 in a subset of bottles), and CH_4 as the sole electron donor and carbon source (see **Supporting Information** for enrichment details). Cultures were transferred into fresh media after Mn(III) was completely reduced to Mn(II), for a total of five transfers over 395 days. By the fourth transfer, cultures with CH_4 headspace (with or without 2% O_2) reduced ~80% of soluble Mn(III) compared to ~30% with N_2 headspace (**Fig. 1**). 16S rRNA gene sequences were dominated by *Betaproteobacteria* (*Rhodocyclales*) and *Deltaproteobacteria* (*Desulfuromonadales*; **Fig. S1)**. $^{13}CH_4$ oxidation to $^{13}CO_2$ was undetectable (**Fig. S2**).

bioRxiv preprint doi: https://doi.org/10.1101/695007; this version posted November 1, 2019. The copyright holder for this preprint (which was not certified by peer review) is the author/funder. All rights reserved. No reuse allowed without permission.

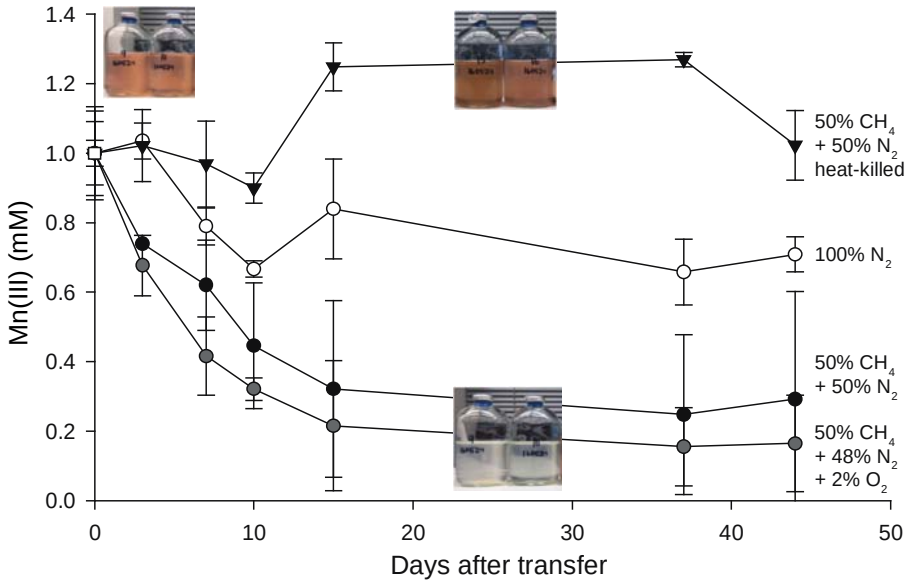

Figure 1. Consumption of Mn(III) in Lake Matano enrichments in the presence and absence of methane. Sediment-free cultures (transfer 4) from 335 days after the initial enrichment were incubated for 45 days with 1 mM Mn(III) pyrophosphate as the sole electron acceptor. Initial bottle headspace contained 50% CH_4 + 50% N_2 (black circles), 50% CH_4+48% N_2+2% O_2 (gray circles), 100% N_2 (white circles), and 50% CH_4+50% N_2 heat killed controls (black triangles). Error bars are standard deviations from duplicate experiments. Color change from red to clear indicates Mn(III) reduction.

Samples for metagenomic and metaproteomic analysis were harvested from the fifth transfer (**Fig. 1; Fig. S1**). Out of 2,952 proteins identified in the proteome, 90% were assigned to *Betaproteobacteria*; of those, 72% mapped to a 99.5% complete metagenome-assembled genome (MAG; *Rhodocyclales* bacterium GT-UBC; NCBI accession QXPY01000000) with 81-82% average nucleotide identity (ANI) and phylogenetic affiliation to *Dechloromonas* spp. (**Table S1; Fig. S3**). This MAG is named here "*Candidatus* Dechloromonas occultata" sp. nov.; etymology: occultata; (L. fem. adj. 'hidden'). The remaining 10% of proteins mapped to *Deltaproteobacteria*; of those, 70% mapped to a nearly complete MAG (*Desulfuromonadales* bacterium GT-UBC; NCBI accession RHLS01000000) with 80% ANI to *Geobacter sulfurreducens*. This MAG is named here "*Candidatus* Geobacter occultata".

bioRxiv preprint doi: https://doi.org/10.1101/695007; this version posted November 1, 2019. The copyright holder for this preprint (which was not certified by peer review) is the author/funder. All rights reserved. No reuse allowed without permission.

Cytochrome expression during Mn(III) reduction. Cytochromes containing multiple *c*-type hemes are key for electron transport during microbial metal transformations, and therefore might also be expected to play a role in Mn(III) reduction. Numerous mono-, di-, and multi (>3)-heme cytochromes (MHCs) were expressed by "*Ca.* D. occultata" in Mn(III)-reducing cultures. Nine out of 15 MHCs encoded by the "*Ca.* D. occultata" MAG were expressed, including two decahemes similar to MtoA in Fe(II)-oxidizing *Betaproteobacteria* (**Tables 1, S2, S3; Figs. 2A, S4).** Several highly expressed MHCs were encoded on a previously unreported 19-gene cluster with 10 cytochrome-*c* proteins, hereafter *occA-S* (**Table 1; Figs. 2B, S5, S6**). OccP was predicted to be an extracellular undecaheme protein of ~100 kDa (922 amino acids). "*Ca.* Dechloromonas occultata" may reduce Mn(III) using the novel extracellular undecaheme OccP as the terminal Mn(III) reductase. Experimental verification of the function of the putative Occ complex is currently limited by the scarcity of genetically tractable *Betaproteobacteria.*

Table 1. Expression levels for "*Ca.* D. occultata" proteins in the presence of CH_4 and N_2. Peptide identifications from mass spectrometry using Comet (Eng et al., 2013) were matched with a metagenome-generated protein database using Prokka (Seemann, 2014), or RAST for bins (Wattam et al., 2013; Overbeek et al., 2014). Database searches were completed on PeptideProphet (Nesvizhskii et al., 2003). Calculated false discovery rates (FDR) were <0.01. Normalized spectral abundances were calculated in QPROT with Abacus (Choi et al., 2015). Peptide counts are normalized to total "*Ca.* D. occultata" proteins x 10,000. Blank cells indicate proteins with <2 normalized peptide counts. Gray boxes indicate membrane proteins that may be underrepresented by mass spectrometry-based metaproteomic analyses, which inherently favor soluble over insoluble membrane-bound or hydrophobic proteins. SP: signal peptide (Y:present/N:absent); TMH: numbers of transmembrane helices; # CxxCH: number of heme-binding motifs; P-sort: predicted cellular location based on Psortb v.3.0. Bold proteins indicate proteins that were significantly more expressed with CH_4 than N_2 ($CH_4/N_2>1$; $p<0.05$). MCP: methyl-accepting chemotaxis protein; PPIase: Peptidyl-proline isomerase; P: periplasm, C: cytoplasm; OM: outer membrane; IM: inner membrane, E: extracellular; U: unknown. MtoX and MtoY were predicted to be an inner membrane cytochrome-b protein and a methyl-accepting chemotaxis protein, respectively.

bioRxiv preprint doi: https://doi.org/10.1101/695007; this version posted November 1, 2019. The copyright holder for this preprint (which was not certified by peer review) is the author/funder. All rights reserved. No reuse allowed without permission.

Enzyme	Function	SP	TMH	CxxCH	P-sort	NCBI ID	Normalized peptide counts				CH4/N2		P value
							CH_4	SD	N_2	SD	ave	SD	
	***Ca.* Dechloromonas occultata**												
Mto-1	MtoX-1 |cyt-b|	N	5	0	IM	RIX49676							
	MtoY-1 |MCP|	N	2	1	IM	RIX49677	2.7	0.5	3.6	0.2	0.8	0.2	0.2
	MtoB-1 |porin|	Y	0	0	OM	RIX49678	10	2	15	2	0.6	0.1	0.004
	MtoA-1	Y	1	10	P	RIX49874	5	1	2.5	0.1	1.9	0.4	0.1
	MtoD-1	N	0	1	P	RIX49875							
Mto-2	MtoX-2 |cyt-b|	N	4	0	IM	RIX48942							
	MtoB-2 |porin|	Y	0	0	OM	RIX48943	8	1	16	0.2	0.5	0.1	0.04
	MtoA-2	Y	1	10	P	RIX48944	7.3	0.8	4	2	2.1	1.3	0.2
	MtoD-2	**Y**	**1**	**1**	**U**	**RIX48945**	**2.6**	**0.3**	**0.7**	**0.3**	**4.0**	**1.4**	**0.003**
Occ	**OccA**	**Y**	**1**	**3**	**P**	**RIX49688**	**4**	**0.5**	**0.7**	**0.6**	**7.8**	**5.7**	**0.01**
	OccB	**Y**	**0**	**3**	**U**	**RIX49689**	**41**	**4**	**19**	**2**	**2.2**	**0.0**	**0.03**
	OccC	N	0	1	U	RIX49877							
	OccD	N	0	3	U	RIX49878							
	OccE |6-NHL|	N	1	0	U	RIX49690	22	2.1	20.5	0.2	1.1	0.1	0.2
	OccF	Y	2	4	E	RIX49691	13	0.7	10.1	0.1	1.3	0.1	0.06
	OccG (PPIase)	**N**	**0**	**0**	**U**	**RIX49692**	**14**	**1**	**3.3**	**0.5**	**4.2**	**0.3**	**0.01**
	OccH	N	0	0	OM/E	RIX49693	6.0	0.2	7.7	0.6	0.8	0.1	0.10
	OccI	N	1	3	U	RIX49694	7	2.5	2.3	0.0	2.9	1.1	0.1
	OccJ	**Y**	**0**	**4**	**U**	**RIX49879**	**44**	**0.2**	**19**	**3**	**2.4**	**0.4**	**0.03**
	OccK	**N**	**0**	**0**	**C**	**RIX49880**	**39**	**6**	**13**	**1**	**3.0**	**0.2**	**0.04**
	OccL	N	1	3	U	RIX49695							
	OccM	N	0	3	U	RIX49881							
	OccN |6 NHL|	N	2	0	U	RIX49696	5.7	0.3	6	1	0.9	0.1	0.2
	OccO |6 NHL|	N	0	0	U	RIX49882	1.2	0.8	4.2	0.4	0.3	0.2	0.03
	OccP	N	0	11	E	RIX49697	14	2	12	3	1.2	0.5	0.4
	OccQ	Y	4	0	IM	RIX49698							
	OccR	N	8	0	IM	RIX49883							
	OccS	N	12	0	IM	RIX49699							
Cyt c	**Cyt c5**	**N**	**1**	**1**	**U**	**RIX47670**	**27**	**2**	**9**	**3**	**3.2**	**0.8**	**0.01**
	Cyt c5	Y	1	2	P	RIX40984	19	2	6	1	3.3	1.0	0.06
	Cyt c'/C_2	Y	1	1	P	RIX44710	17	5	3.6	0.8	4.8	2.3	0.09
	Cyt c'/C_2	Y	1	1	P	RIX49630	7	1	1.2	0.9	8.2	6.6	0.07
	Cyt c551/c552	Y	0	1	P	RIX49087	13	3	2.8	0.0	4.8	1.1	0.06
	Cyt c4	Y	0	2	P	RIX48804	16	0.8	9.8	0.8	1.6	0.2	0.06
	Cyt c4	Y	0	2	P	RIX44782	4	2	1.7	0.7	2.6	0.1	0.08
	Cyt c4	**Y**	**0**	**2**	**P**	**RIX45018**	**7**	**0.6**	**2.2**	**0.2**	**3.0**	**0.0**	**0.02**
Nap	NapA	Y	0	0	P	RIX41011	76	2	67	3	1.1	0.1	0.1
	NapB	**Y**	**1**	**2**	**P**	**RIX41010**	**15**	**1**	**5**	**2**	**3.2**	**0.9**	**0.02**
	NapC	N	1	4	IM	RIX41009	12	3	13	1	1.0	0.2	0.1
Nir	NirS	Y	0	1	P	RIX44719	58	2	44	4	1.3	0.2	0.1
	NirB	Y	1	2	P	RIX44720	14	3	10	2	1.5	0.6	0.2
	NirC	N	0	1	P	RIX44788							
	NirF	Y	1	0	P or C	RIX44721	2	1	7	1	0.3	0.1	0.02
Nor	NorC	N	1	1	IM	RIX45182	3.5	0.7	3.2	0.7	1.1	0.0	0.1
	NorB	N	12	1	IM	RIX45183							
cNos	cNosZ	Y	0	0	P	RIX42539	77	17	66	8	1.2	0.3	0.2
	cNosC1	Y	1	1	P	RIX42538	16	2	4	2	5	3	0.08
	cNosC2	**Y**	**1**	**2**	**P**	**RIX42537**	**10**	**0.1**	**3.9**	**0.3**	**2.6**	**0.1**	**0.02**
	cNosB	N	6	0	IM	RIX42536							
	cNosD	N	0	0	P	RIX42535							
	cNosG	N	1	0	C	RIX42534							
	cNosH	N	4	0	IM	RIX42533							
Qcr	QcrA	N	9	0	CM	RIX41976							
	QcrB	N	9	0	CM	RIX41977							
	QcrC	N	1	0	CM	RIX41978							
Proteases	Serine protease	N	0	0	P	RIX49468	27	2	1.0	0.3	29	10	0.02
	Carboxyl-terminal protease (S41)	N	1	0	CM	RIX48818	18.5	0.8	8.0	0.9	2.3	0.1	0.0002
Membrane/Extracellular	DUF4214 protein	N	0	0	OM/E	RIX44180	146	25	43	0.6	3.4	0.5	0.05
	S-layer protein	N	0	0	U	RIX44181	8	0.5	10	0.6	0.8	0.1	0.14
	PEP-CTERM sorting	Y	1	0	E	RIX45463	68	6	33	10	2.1	0.5	0.03
	Tol-Pal system protein TolB	Y	0	0	P	RIX44015	20	2	12	1	1.67	0.05	0.03
	Peptidoglycan-associated lipoprotein (Pal)	N	0	0	OM	RIX44016	27.3	0.2	10	3	3	1	0.04
	Tol-Pal system protein YbgF	Y	0	0	U	RIX44017	10.8	0.4	4	2	4	2	0.06
	Pilus assembly protein	N	0	0	U	RIX46961	54	5	30	5	1.8	0.1	0.001
Other	PQQ-dependent dehydrogenase	Y	0	0	P	RIX45050	37	4	17	1	2.2	0.1	0.03
	Phasin family granule-associated protein	N	0	0	U	RIX40682	49	2	22	1	2.2	0.2	0.03
	Phasin family granule-associated protein	Y	0	0	U	RIX40683	34	4	16	1	2.1	0.0	0.03
	High potential iron-sulfur protein	Y	0	0	U	RIX49681	10.79	0.01	6.5	0.4	1.7	0.1	0.02
	Electron transfer flavoprotein (FixA)	N	0	0	C	RIX43544	16	3	10	2	1.7	0.0	0.04
	***Ca.* Geobacter occultata**												
E-pilus	Type IV pilin PilA	N	1	0	E	RNC67631	93	3	18	3	5	1	0.02

Proteins with 40-60% identity to the expressed "*Ca.* D. occultata" OccP protein were widely distributed in *Betaproteobacteria* from diverse freshwaters and deep subsurface groundwaters, as well as several *Gammaproteobacteria* and one alphaproteobacterium (**Fig. 2D; Table S3).** Most *occP*-containing bacteria also possessed *mtoA* and denitrification genes (**Fig. 2D**; **Figs. S7**, **S8)**. These results widen the phylogenetic and structural diversity of candidate extracellular MHCs that may be involved in microbial Mn(III) reduction.

bioRxiv preprint doi: https://doi.org/10.1101/695007; this version posted November 1, 2019. The copyright holder for this preprint (which was not certified by peer review) is the author/funder. All rights reserved. No reuse allowed without permission.

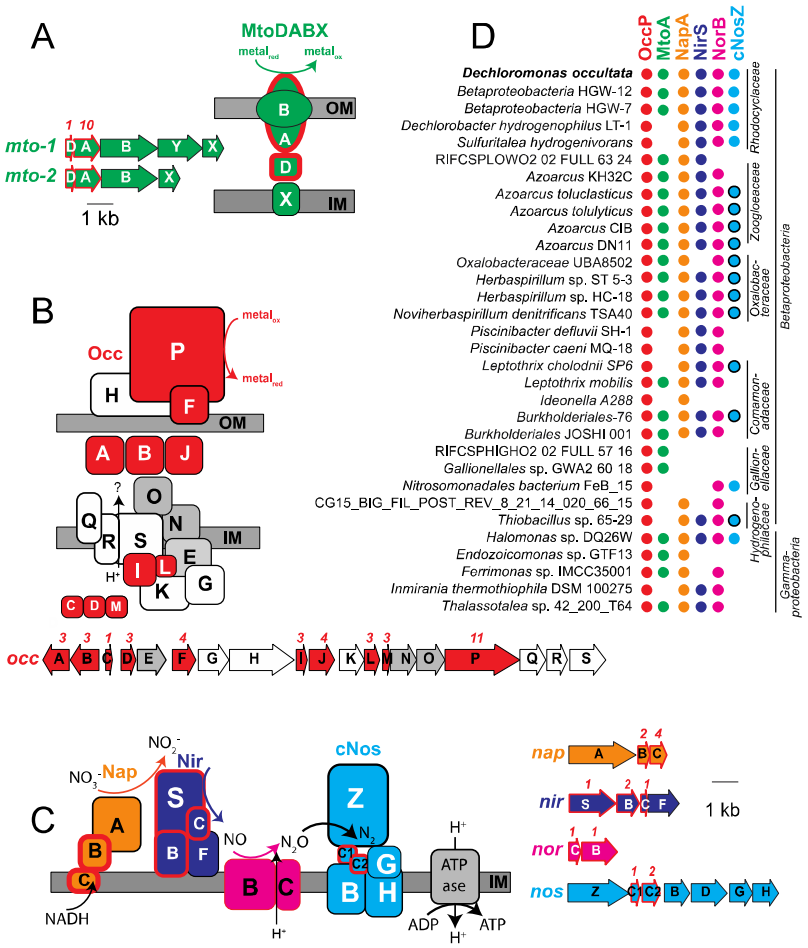

Figure 2. Gene arrangement, predicted protein location, and taxonomic distribution of major expressed respiratory complexes in "*Ca*. D. occultata". A: MtoDAB(Y)X porin-cytochrome c electron conduit; **B:** OccA-S; **C:** denitrification complexes (Nap, Nir, Nor and cNos); **D:** Occurrence of key marker genes in *Betaproteobacteria* and *Gammaproteobacteria* with >95% complete genomes that encode OccP. Protein sequences from "*Ca*. D. occultata" were used as query against a genome database and searched using PSI BLAST. Matches with identities >40%, query coverage >80% and E values $<10^{-5}$ were considered positive. Red fill around genes and proteins indicate cytochrome-*c* proteins. Black outlines around blue circles in D indicate type I nitrous oxide reductase to distinguish from blue dots (type II/cytochrome-nitrous oxide reductase). Gray-shaded genes on the *occ* gene cluster indicate 6-NHL repeat proteins. Protein locations shown are based on P-sort predictions. Numbers above genes indicate number of CxxCH motifs predicted to bind cytochrome *c*. IM: inner membrane; OM: outer membrane. For more details, see **Table 1** and **Table S3.**

***Heme-copper oxidases in* "Ca. *D. occultata*".** "*Ca*. D. occultata" expressed high-affinity cbb_3-type cytochrome c oxidase (CcoNOQP) associated with microaerobic respiration (**Table S4).** Features of the "*Ca*. D. occultata" *occS* gene product, including conserved histidine residues (H-94, H-411, and H-413) that bind hemes a and a_3, as well as the H-276 residue that binds Cu_B (**Fig. S6**), suggest that OccS may function similarly to CcoN, the terminal heme-copper oxidase proton pump in aerobic respiration. All identified OccS amino acid sequences lack Cu_B ligands

bioRxiv preprint doi: https://doi.org/10.1101/695007; this version posted November 1, 2019. The copyright holder for this preprint (which was not certified by peer review) is the author/funder. All rights reserved. No reuse allowed without permission.

Y-280 and H-403, and most lack Cu_B ligands H-325 and H-326. OccS sequences also lack polar and ionizable amino acids that comprise the well-studied D and K channels involved in proton translocation in characterized cytochrome c oxidases (Blomberg and Siegbahn, 2014), but contain conserved H, C, E, D, and Y residues that may serve as alternate proton translocation pathways, similar to those recently discovered in qNOR (Gonska et al., 2018). OccS homologs were also found in *Azoarcus* spp. and deep subsurface *Betaproteobacteria* (**Fig. S6**).

Expression of denitrification proteins and possible sources of oxidized nitrogen species.

Periplasmic nitrate reductase (NapA), cytochrome nitrite reductase (NirS), and type II atypical nitrous oxide reductase (cNosZ; **Fig. S7**) were highly expressed by "*Ca.* D. occultata" **(Table 1)**. Expression of the denitrification pathway was not expected because oxidized nitrogen species were not added to the medium, to which the only nitrogen supplied was NH_4Cl (0.2 mM) and N_2 in the headspace. Nitrification genes were not found in the metagenome. Because solid-phase Mn(III) is known to chemically oxidize NH_4^+ (Aigle et al., 2017; Boumaiza et al., 2018), we tested for abiotic NH_4^+ oxidation by soluble Mn(III) (1 mM). Ammonium concentrations remained unchanged, and no N_2O or NO_x^- production was observed (**Fig. S8**), likely because our experiments lacked solid surfaces to mediate electron transfer. These findings are consistent with lack of detectable ammonium oxidation by Mn(III) pyrophosphate in estuarine sediments (Crowe et al., 2012). The close redox potential of Mn^{3+}-pyrophosphate (~0.8 V; Yamaguchi and Sawyer, 1985)) to oxidized nitrogen species (0.35-0.75 V at circumneutral pH) and the lack of oxygen in the media could have induced the expression of denitrification genes simultaneously with Mn(III)-reduction genes. *Gammaproteobacteria*, for example, reduce Mn(III) even in the presence of nitrate (Kostka et al., 1995).

bioRxiv preprint doi: https://doi.org/10.1101/695007; this version posted November 1, 2019. The copyright holder for this preprint (which was not certified by peer review) is the author/funder. All rights reserved. No reuse allowed without permission.

Carbon metabolism. "*Ca.* D. occultata" appeared to be growing mixotrophically. It expressed two CO_2-assimilation pathways, a modified Calvin-Benson-Bassham (CBB) pathway, an open 3-hydroxypropionate (3-HP) pathway, the oxidative TCA cycle (including citrate synthase and 2-oxoglutarate dehydrogenase), and organic carbon transporters (**Table S4; Fig. S9)**. Like *D. agitata* and *D. denitrificans*, the CBB pathway of "*Ca.* D. occultata" did not encode RuBisCO and sedoheptulose-1,7-bisphosphatase (SHbisPase; **Fig. S10)**; SHbisPase may be replaced by 6-phosphofructokinase and an energy-generating pyrophosphatase (RIX41248; Kleiner et al., 2012; Zorz et al., 2018). A hypothetical signal peptide-containing protein (RIX43053) in between fructose-bisphosphatase and transkelotase was more highly expressed during growth on CH_4 vs. N_2. "*Ca.* D. occultata" also encodes citrate lyase and 2-oxoglutarate/ferredoxin oxidoreductase indicative of a reductive TCA cycle, but these enzymes were not detected in the proteomic data.

Methane stimulated Mn(III) reduction and cytochrome expression in "*Ca*. D. occultata" enrichment cultures. However, we did not detect isotopically labeled CO_2 (**Fig. S2**) and proteomic evidence of carbon assimilation indicated that "*Ca*. D. occultata" assimilated organic carbon and not one-carbon compounds. "*Ca*. D. occultata" also expressed a PQQ-dependent methanol/ethanol dehydrogenase at higher levels in the presence of CH_4 than N_2 ($p=0.03$; **Table 1**). A PQQ-methanol dehydrogenase has been implicated in methylotrophy in *Rhodocyclales* (Kalyuzhnaya et al., 2008). Our search for any other genes that could encode proteins capable of CH_4 oxidation recovered a cytochrome P450 (RIX47519) with 42% identity to *Methylobacterium organophilum*, which is capable of methanotrophy by an unknown mechanism (Green and Bousfield, 1983; Dedysh et al., 2004; Van Aken et al., 2004). Oxidation

bioRxiv preprint doi: https://doi.org/10.1101/695007; this version posted November 1, 2019. The copyright holder for this preprint (which was not certified by peer review) is the author/funder. All rights reserved. No reuse allowed without permission.

of methane to methanol by cytochrome P450 or another enzyme would serve as a substrate for pyrroloquinoline quinone (PQQ)-methanol dehydrogenase. However, RIX47519 was undetected in the proteomic data.

While the specific role of CH_4 in Mn(III) reduction remains unknown, CH_4 appeared to significantly stimulate expression of many cytochrome *c* proteins, including OccABGJK, MtoD-2, and cytochrome-*c*4 and -*c*5 proteins associated with anaerobic respiration ($p < 0.05$; **Table 1; Fig. 2C**). Expression of several "*Ca.* D. occultata" proteins involved in outer membrane structure and composition, including an extracellular DUF4214 protein located next to an S-layer protein similar to those involved in manganese binding and deposition (Wang et al., 2009), a serine protease possibly involved in Fe(III) particle attachment (Burns et al., 2009), an extracellular PEP-CTERM sorting protein for protein export (Haft et al., 2006), and a Tol-Pal system for outer membrane integrity, were also higher in the presence of CH_4 (**Table 1)**. Lack of proteomic and isotopic evidence for use of CH_4 as an electron donor suggests that CH_4 may be indirectly involved in Mn(III) reduction in "*Ca*. D. occultata", possibly by lowering the redox potential of the cultures to favor higher rates of Mn(III) reduction than in N_2-only cultures.

Transporters and sensors. Numerous transporters were present in the "*Ca*. D. occultata" genome, including 26 TonB-dependent siderophore transporters, 13 TRAP transporters for dicarboxylate transport, as well as ABC transporters for branched-chained amino acids and dipeptides and polypeptides (**Table S4**). "*Ca*. D. occultata" also contained a large number of environmental sensing genes: 52 bacterial hemoglobins with PAS-PAC sensors, 8 TonB-dependent receptors, and 8 NO responsive regulators (Dnr: Crp/fr family; **Table S4**). Uniquely in "*Ca*. D. occultata", PAC-PAS sensors flanked accessory genes *nosFLY* on the *c-nosZ* operon

bioRxiv preprint doi: https://doi.org/10.1101/695007; this version posted November 1, 2019. The copyright holder for this preprint (which was not certified by peer review) is the author/funder. All rights reserved. No reuse allowed without permission.

(**Fig. S7**). Comparison of these flanking PAC-PAS sensors in "*Ca*. D. occultata" with O_2-binding sensors revealed that an arginine ~20 aa upstream from the conserved histidine as the distal pocket ligand for O_2-binding is not present in either sensor (**Fig. S11**), suggesting that the sensor may bind a different ligand, possibly NO, consistent with the placement of these genes next to cNosZ (Shimizu et al., 2015).

Nutrient storage. Active synthesis of storage polymers suggested that "*Ca*. D. occultata" was experiencing electron acceptor starvation at the time of harvesting, consistent with Mn(III) depletion in the bottles (Liu et al., 2015; Guanghuan et al., 2018). Polyphosphate-related proteins, including phosphate transporters, polyphosphate kinase, polyphosphatase, and poly-3-hydroxybutyrate synthesis machinery were detected in the proteome (**Table S4**). Polyphosphate-accumulating organisms store polyphosphates with energy generated from organic carbon oxidation during aerobic respiration or denitrification, which are later hydrolyzed when respiratory electron acceptors for ATP production are limiting. Cyanophycin was being actively synthesized for nitrogen storage.

Geobacter. "*Ca*. G. occultata" expressed genes involved in the TCA cycle and subsequent pathways for energy-generation included citrate synthase, malate dehydrogenase, isocitrate dehydrogenase, fumarate hydratase and NADH-ubiquinone oxidoreductase at moderate abundance. "*Ca.* Geobacter occultata" contained 17 multiheme c-type cytochromes, none of which were detected in the proteome. The lack of expression of electron transport and metal-reducing pathways makes it unlikely that "*Ca.* Geobacter occultata" was solely responsible for Mn(III) reduction observed in the incubations. It is possible that "*Ca.* G. occultata" and "*Ca*. D. occultata" engage in direct interspecies electron transport via e-pilins. A type IV pilin with 87%

bioRxiv preprint doi: https://doi.org/10.1101/695007; this version posted November 1, 2019. The copyright holder for this preprint (which was not certified by peer review) is the author/funder. All rights reserved. No reuse allowed without permission.

identity to *Geobacter pickeringii* (Holmes et al., 2016) was significantly more highly expressed with CH_4 vs. N_2 in the "*Ca*. G. occultata" proteome (p=0.02; Table 1). The possible involvement of *Geobacter* e-pilins in Mn(III) reduction remains an open question, due to the lack of studies examining the possibility of Mn(III) reduction in *Deltaproteobacteria*.

Conclusions. To our knowledge, this study provides the first evidence for biological reduction of soluble Mn(III) by a bacterium outside of the *Gammaproteobacteria* class. The dominant bacterium in Mn(III)-reducing enrichment cultures was "*Ca*. D. occultata", a member of the *Rhodocyclales* order of *Betaproteobacteria*. "*Ca*. D. occultata" expressed decahemes similar to the Mto pathway, and *occ* genes, including a novel extracellular undecaheme (OccP), which are predicted to encode a new respiratory electron transport pathway. The novel *occ* operon was found to be widespread in *Betaproteobacteria* from the deep subsurface, where metal cycling can fuel microbial metabolism.

Puzzles remain about whether "*Ca*. D. occultata" can transform two potent greenhouse gases: methane and nitrous oxide. Although "*Ca*. D. occultata" was enriched with methane as the sole electron donor and cultures reduced Mn(III) more rapidly in the presence of CH_4, no CH_4 oxidation activity was measured in Mn(III)-reducing cultures, and proteomic data suggested that "*Ca*. D. occultata" was growing mixotrophically rather than assimilating CH_4. It is possible than CH_4 played an indirect role in Mn(III) reduction, perhaps by lowering the redox state of the cultures to conditions that were more favorable for anaerobic Mn(III) respiration. Further, although we did not add oxidized nitrogen compounds to our media, and Mn(III) did not chemically oxidize NH_4^+ under our culture conditions, type II nitrous oxide reductase (cNosZ) was one of the most abundant proteins expressed in Mn(III)-reducing cultures. The role of

bioRxiv preprint doi: https://doi.org/10.1101/695007; this version posted November 1, 2019. The copyright holder for this preprint (which was not certified by peer review) is the author/funder. All rights reserved. No reuse allowed without permission.

cNosZ and other denitrification enzymes in "*Ca*. D. occultata" metabolism, and their possible connection to Mn(III) reduction, remain to be investigated.

Acknowledgements. This research was funded by NASA Exobiology grant NNX14AJ87G. Support was also provided by a Center for Dark Energy Biosphere Investigations (NSF-CDEBI OCE-0939564) small research grant and supported by the NASA Astrobiology Institute (NNA15BB03A) and a NASA Astrobiology Postdoctoral Fellowship to NS. SAC was supported through NSERC CRC, CFI, and Discovery grants. We thank Marcus Bray, Andrew Burns, Caleb Easterly, Pratik Jagtap, Cory Padilla, Angela Peña, Johnny Striepen, and Rowan Wolschleger for technical assistance. We thank Emily Weinert for helpful discussions.

Competing Interests: The authors declare no competing interests.

bioRxiv preprint doi: https://doi.org/10.1101/695007; this version posted November 1, 2019. The copyright holder for this preprint (which was not certified by peer review) is the author/funder. All rights reserved. No reuse allowed without permission.

References

Aigle, A., Bonin, P., Iobbi-Nivol, C., Mejean, V., and Michotey, V. (2017) Physiological and transcriptional approaches reveal connection between nitrogen and manganese cycles in *Shewanella algae* C6G3. *Sci Rep* **7**: 44725.

Anantharaman, K., Brown, C.T., Hug, L.A., Sharon, I., Castelle, C.J., Probst, A.J., Thomas, B.C., Singh, A., Wilkins, M.J., Karaoz, U., Brodie, E.L., Williams, K.H., Hubbard, S.S., and Banfield, J.F. (2016) Thousands of microbial genomes shed light on interconnected biogeochemical processes in an aquifer system. *Nat Commun* **7**: 13219.

Beal, E.J., House, C.H., and Orphan, V.J. (2009) Manganese- and iron-dependent marine methane oxidation. *Science* **325**: 184-187.

Blomberg, M.R., and Siegbahn, P.E. (2014) Proton pumping in cytochrome c oxidase: Energetic requirements and the role of two proton channels. *Biochim Biophys Acta* **1837**: 1165-1177.

Boumaiza, H., Coustel, R., Despas, C., Ruby, C., and Bergaoui, L. (2018) Interaction of ammonium with birnessite: Evidence of a chemical and structural transformation in alkaline aqueous medium. *J Solid State Chem* **258**: 543-550.

Burns, J.L., Ginn, B.R., Bates, D.J., Dublin, S.N., Taylor, J.V., Apkarian, R.P., Amaro-Garcia, S., Neal, A.L., and DiChristina, T.J. (2009) Outer membrane-associated serine protease involved in adhesion of *Shewanella oneidensis* to Fe(III) oxides. *Environ Sci Technol* **44**: 68-73.

Choi, H., Kim, S., Fermin, D., Tsou, C.-C., and Nesvizhskii, A.I. (2015) QPROT: Statistical method for testing differential expression using protein-level intensity data in label-free quantitative proteomics. *J Proteomics* **129**: 121-126.

Crowe, S.A., Canfield, D.E., Mucci, A., Sundby, B., and Maranger, R. (2012) Anammox, denitrification and fixed-nitrogen removal in sediments from the Lower St. Lawrence Estuary. *Biogeosciences* **9**: 4309-4321.

Crowe, S.A., Katsev, S., Leslie, K., Sturm, A., Magen, C., Nomosatryo, S., Pack, M.A., Kessler, J.D., Reeburgh, W.S., Roberts, J.A., Gonzalez, L., Douglas Haffner, G., Mucci, A., Sundby, B., and Fowle, D.A. (2011) The methane cycle in ferruginous Lake Matano. *Geobiology* **9**: 61-78.

Cummings, D.E., Caccavo, F., Spring, S., and Rosenzweig, R.F. (1999) Ferribacterium limneticum, gen. nov., sp. nov., an Fe(III)-reducing microorganism isolated from mining-impacted freshwater lake sediments. *Arch Microbiol* **171**: 183-188.

Dedysh, S.N., Dunfield, P.F., and Trotsenko, Y.A. (2004) Methane utilization by *Methylobacterium* species: new evidence but still no proof for an old controversy. *Int J Syst Evol Microbiol* **54**: 1919-1920.

Edwards, M.J., Hall, A., Shi, L., Fredrickson, J.K., Zachara, J.M., Butt, J.N., Richardson, D.J., and Clarke, T.A. (2012) The crystal structure of the extracellular 11-heme cytochrome UndA reveals a conserved 10-heme motif and defined binding site for soluble iron chelates. *Structure* **20**: 1275-1284.

Emerson, D., Field, E.K., Chertkov, O., Davenport, K.W., Goodwin, L., Munk, C., Nolan, M., and Woyke, T. (2013) Comparative genomics of freshwater Fe-oxidizing bacteria: implications for physiology, ecology, and systematics. *Front Microbiol* **4**: 254.

bioRxiv preprint doi: https://doi.org/10.1101/695007; this version posted November 1, 2019. The copyright holder for this preprint (which was not certified by peer review) is the author/funder. All rights reserved. No reuse allowed without permission.

Eng, J.K., Jahan, T.A., and Hoopmann, M.R. (2013) Comet: an open□source MS/MS sequence database search tool. *Proteomics* **13**: 22-24.

Finneran, K.T., Johnsen, C.V., and Lovley, D.R. (2003) *Rhodoferax ferrireducens* sp. nov., a psychrotolerant, facultatively anaerobic bacterium that oxidizes acetate with the reduction of Fe(III). *Int J Syst Evol Microbiol* **53**: 669-673.

Fredrickson, J.K., Romine, M.F., Beliaev, A.S., Auchtung, J.M., Driscoll, M.E., Gardner, T.S., Nealson, K.H., Osterman, A.L., Pinchuk, G., and Reed, J.L. (2008) Towards environmental systems biology of *Shewanella*. *Nat Rev Microbiol* **6**: 592.

Gonska, N., Young, D., Yuki, R., Okamoto, T., Hisano, T., Antonyuk, S., Hasnain, S.S., Muramoto, K., Shiro, Y., and Tosha, T. (2018) Characterization of the quinol-dependent nitric oxide reductase from the pathogen *Neisseria meningitidis*, an electrogenic enzyme. *Sci Rep* **8**: 3637.

Green, P.N., and Bousfield, I.J. (1983) Emendation of *Methylobacterium* Patt, Cole, and Hanson 1976; *Methylobacterium rhodinum* (Heumann 1962) comb. nov. corrig.; *Methylobacterium radiotolerans* (Ito and Iizuka 1971) comb. nov. corrig.; and *Methylobacterium mesophilicum* (Austin and Goodfellow 1979) comb. nov. *Int J Syst Evol Microbiol* **33**: 875-877.

Guanghuan, G., Jianqiang, Z., Aixia, C., Bo, H., Ying, C., Kun, G., Xiaoling, L., and Xiaoqian, D. (2018) Nitrogen removal and nitrous oxide emission in an anaerobic/oxic/anoxic sequencing biofilm Batch reactor. *Environ Eng Sci* **35**: 19-26.

Haft, D.H., Paulsen, I.T., Ward, N., and Selengut, J.D. (2006) Exopolysaccharide-associated protein sorting in environmental organisms: the PEP-CTERM/EpsH system. Application of a novel phylogenetic profiling heuristic. *BMC Biol* **4**: 29.

He, S., Barco, R.A., Emerson, D., and Roden, E.E. (2017) Comparative genomic analysis of neutrophilic iron(II) oxidizer genomes for candidate genes in extracellular electron transfer. *Front Microbiol* **8**.

Heintze, S., and Mann, P. (1947) Soluble complexes of manganic manganese. *J Agric Sci* **37**: 23-26.

Hernsdorf, A.W., Amano, Y., Miyakawa, K., Ise, K., Suzuki, Y., Anantharaman, K., Probst, A., Burstein, D., Thomas, B.C., and Banfield, J.F. (2017) Potential for microbial H2 and metal transformations associated with novel bacteria and archaea in deep terrestrial subsurface sediments. *ISME J* **11**: 1915-1929.

Holmes, D.E., Dang, Y., Walker, D.J., and Lovley, D.R. (2016) The electrically conductive pili of *Geobacter* species are a recently evolved feature for extracellular electron transfer. *Microb Genom* **2**.

Jones, C., Crowe, S.A., Sturm, A., Leslie, K.L., MacLean, L.C.W., Katsev, S., Henny, C., Fowle, D.A., and Canfield, D.E. (2011) Biogeochemistry of manganese in ferruginous Lake Matano, Indonesia. *Biogeosciences* **8**: 2977-2991.

Kalyuzhnaya, M.G., Hristova, K.R., Lidstrom, M.E., and Chistoserdova, L. (2008) Characterization of a novel methanol dehydrogenase in representatives of Burkholderiales: Implications for environmental detection of methylotrophy and evidence for convergent evolution. *J Bacteriol* **190**: 3817-3823.

bioRxiv preprint doi: https://doi.org/10.1101/695007; this version posted November 1, 2019. The copyright holder for this preprint (which was not certified by peer review) is the author/funder. All rights reserved. No reuse allowed without permission.

359 Kato, S., Ohkuma, M., Powell, D.H., Krepski, S.T., Oshima, K., Hattori, M., Shapiro, N., Woyke, T., and
360 Chan, C.S. (2015) Comparative genomic insights into ecophysiology of neutrophilic, microaerophilic iron
361 oxidizing bacteria. *Front Microbiol* **6**: 1265.

362 Kleiner, M., Wentrup, C., Lott, C., Teeling, H., Wetzel, S., Young, J., Chang, Y.-J., Shah, M.,
363 VerBerkmoes, N.C., Zarzycki, J., Fuchs, G., Markert, S., Hempel, K., Voigt, B., Becher, D., Liebeke, M.,
364 Lalk, M., Albrecht, D., Hecker, M., Schweder, T., and Dubilier, N. (2012) Metaproteomics of a gutless
365 marine worm and its symbiotic microbial community reveal unusual pathways for carbon and energy use.
366 *Proc Natl Acad Sci* **109**: 1173-1182.

367 Kostka, J.E., Luther, G.W., and Nealson, K.H. (1995) Chemical and biological reduction of Mn(III)-
368 pyrophosphate complexes - potential importance of dissolved Mn(III) as an environmental oxidant.
369 *Geochim Cosmochim Acta* **59**: 885-894.

370 Liu, Y., Peng, L., Guo, J., Chen, X., Yuan, Z., and Ni, B.-J. (2015) Evaluating the role of microbial
371 internal storage turnover on nitrous oxide accumulation during denitrification. *Sci Rep* **5**: 15138.

372 Madison, A.S., Tebo, B.M., Mucci, A., Sundby, B., and Luther, G.W., 3rd (2013) Abundant porewater
373 Mn(III) is a major component of the sedimentary redox system. *Science* **341**: 875-878.

374 Nesvizhskii, A.I., Keller, A., Kolker, E., and Aebersold, R. (2003) A statistical model for identifying
375 proteins by tandem mass spectrometry. *Anal Chem* **75**: 4646-4658.

376 Oldham, V.E., Siebecker, M.G., Jones, M.R., Mucci, A., Tebo, B.M., and Luther, G.W. (2019) The
377 speciation and mobility of Mn and Fe in estuarine sediments. *Aquat Geochem* **25**: 3-26.

378 Overbeek, R., Olson, R., Pusch, G.D., Olsen, G.J., Davis, J.J., Disz, T., Edwards, R.A., Gerdes, S.,
379 Parrello, B., Shukla, M., Vonstein, V., Wattam, A.R., Xia, F., and Stevens, R. (2014) The SEED and the
380 Rapid Annotation of microbial genomes using Subsystems Technology (RAST). *Nucleic Acids Res* **42**:
381 D206-214.

382 Richardson, D.J., Butt, J.N., Fredrickson, J.K., Zachara, J.M., Shi, L., Edwards, M.J., White, G., Baiden,
383 N., Gates, A.J., and Marritt, S.J. (2012) The 'porin–cytochrome' model for microbe□to□mineral electron
384 transfer. *Mol Microbiol* **85**: 201-212.

385 Riedinger, N., Formolo, M.J., Lyons, T.W., Henkel, S., Beck, A., and Kasten, S. (2014) An inorganic
386 geochemical argument for coupled anaerobic oxidation of methane and iron reduction in marine
387 sediments. *Geobiology* **12**: 172-181.

388 Seemann, T. (2014) Prokka: rapid prokaryotic genome annotation. *Bioinformatics* **30**: 2068-2069.

389 Shi, L., Belchik, S.M., Wang, Z., Kennedy, D.W., Dohnalkova, A.C., Marshall, M.J., Zachara, J.M., and
390 Fredrickson, J.K. (2011) Identification and characterization of UndAHRCR-6, an outer membrane
391 endecaheme c-type cytochrome of *Shewanella* sp. strain HRCR-6. *Appl Environ Microbiol* **77**: 5521-
392 5523.

393 Shi, L., Dong, H., Reguera, G., Beyenal, H., Lu, A., Liu, J., Yu, H.-Q., and Fredrickson, J.K. (2016)
394 Extracellular electron transfer mechanisms between microorganisms and minerals. *Nat Rev Microbiol* **14**:
395 651.

bioRxiv preprint doi: https://doi.org/10.1101/695007; this version posted November 1, 2019. The copyright holder for this preprint (which was not certified by peer review) is the author/funder. All rights reserved. No reuse allowed without permission.

396 Shimizu, T., Huang, D., Yan, F., Stranava, M., Bartosova, M., Fojtíková, V., and Martínková, M.t. (2015)
397 Gaseous O2, NO, and CO in signal transduction: structure and function relationships of heme-based gas
398 sensors and heme-redox sensors. *Chem Rev* **115**: 6491-6533.

399 Smith, J.A., Lovley, D.R., and Tremblay, P.L. (2013) Outer cell surface components essential for Fe(III)
400 oxide reduction by Geobacter metallireducens. *Appl Environ Microbiol* **79**: 901-907.

401 Szeinbaum, N., Burns, J.L., and DiChristina, T.J. (2014) Electron transport and protein secretion
402 pathways involved in Mn(III) reduction by Shewanella oneidensis. *Environ Microbiol Rep* **6**: 490-500.

403 Szeinbaum, N., Lin, H., Brandes, J.A., Taillefert, M., Glass, J.B., and DiChristina, T.J. (2017) Microbial
404 manganese(III) reduction fuelled by anaerobic acetate oxidation. *Environ Microbiol* **19**: 3475-3486.

405 Van Aken, B., Peres, C.M., Doty, S.L., Yoon, J.M., and Schnoor, J.L. (2004) *Methylobacterium populi*
406 sp. nov., a novel aerobic, pink-pigmented, facultatively methylotrophic, methane-utilizing bacterium
407 isolated from poplar trees (Populus deltoides×nigra DN34). *Int J Syst Evol Microbiol* **54**: 1191-1196.

408 Wang, X., Schröder, H.C., Schloßmacher, U., and Müller, W.E. (2009) Organized bacterial assemblies in
409 manganese nodules: evidence for a role of S-layers in metal deposition. *Geo-Marine Letters* **29**: 85-91.

410 Wattam, A.R., Abraham, D., Dalay, O., Disz, T.L., Driscoll, T., Gabbard, J.L., Gillespie, J.J., Gough, R.,
411 Hix, D., and Kenyon, R. (2013) PATRIC, the bacterial bioinformatics database and analysis resource.
412 *Nucleic Acids Res* **42**: D581-D591.

413 Yamaguchi, K.S., and Sawyer, D.T. (1985) The redox chemistry of manganese(III) and manganese(IV)
414 complexes. *Isr J Chem* **25**: 164-176.

415 Yang, Y., Chen, J., Qiu, D., and Zhou, J. (2013) Roles of UndA and MtrC of *Shewanella putrefaciens*
416 W3-18-1 in iron reduction. *BMC Microbiol* **13**: 267.

417 Zorz, J.K., Kozlowski, J.A., Stein, L.Y., Strous, M., and Kleiner, M. (2018) Comparative proteomics of
418 three species of ammonia-oxidizing bacteria. *Front Microbiol* **9**: 938.

419
420

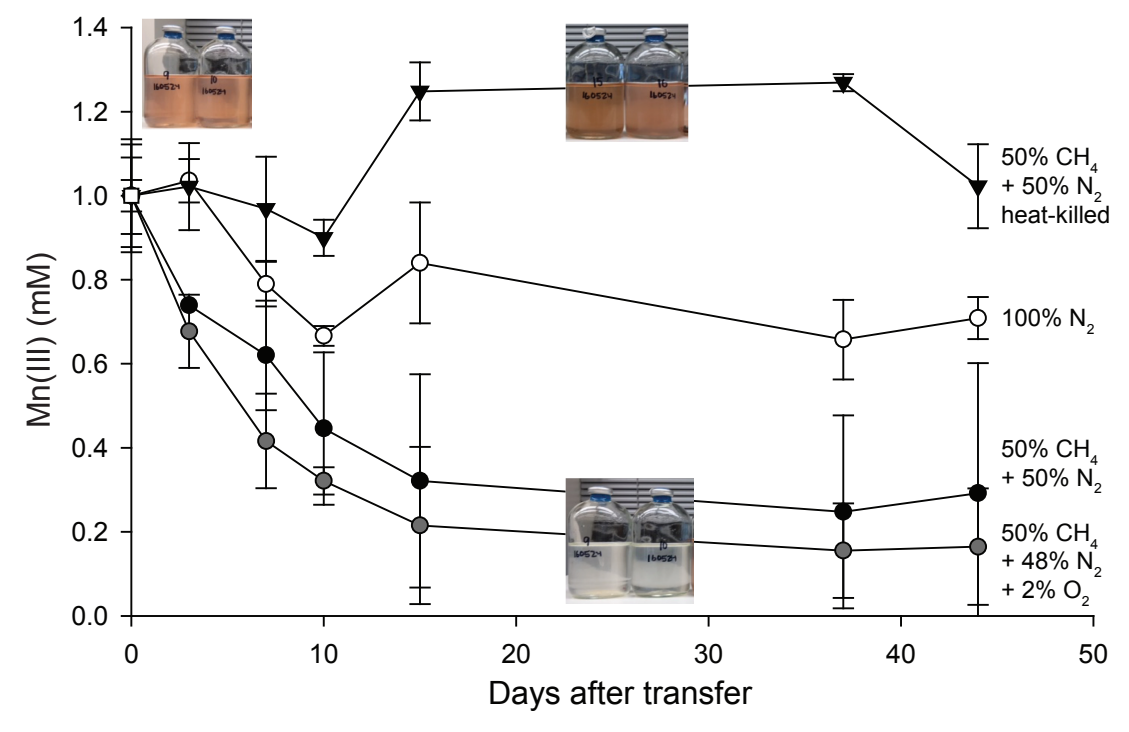
Mn(III) (mM)
1.4
1.2
1.0
0.8
0.6
0.4
0.2
0.0
0
10
20
30
40
50
Days after transfer
50% CH4 + 50% N2 heat-killed
100% N2
50% CH4 + 50% N2
50% CH4 + 48% N2 + 2% O2

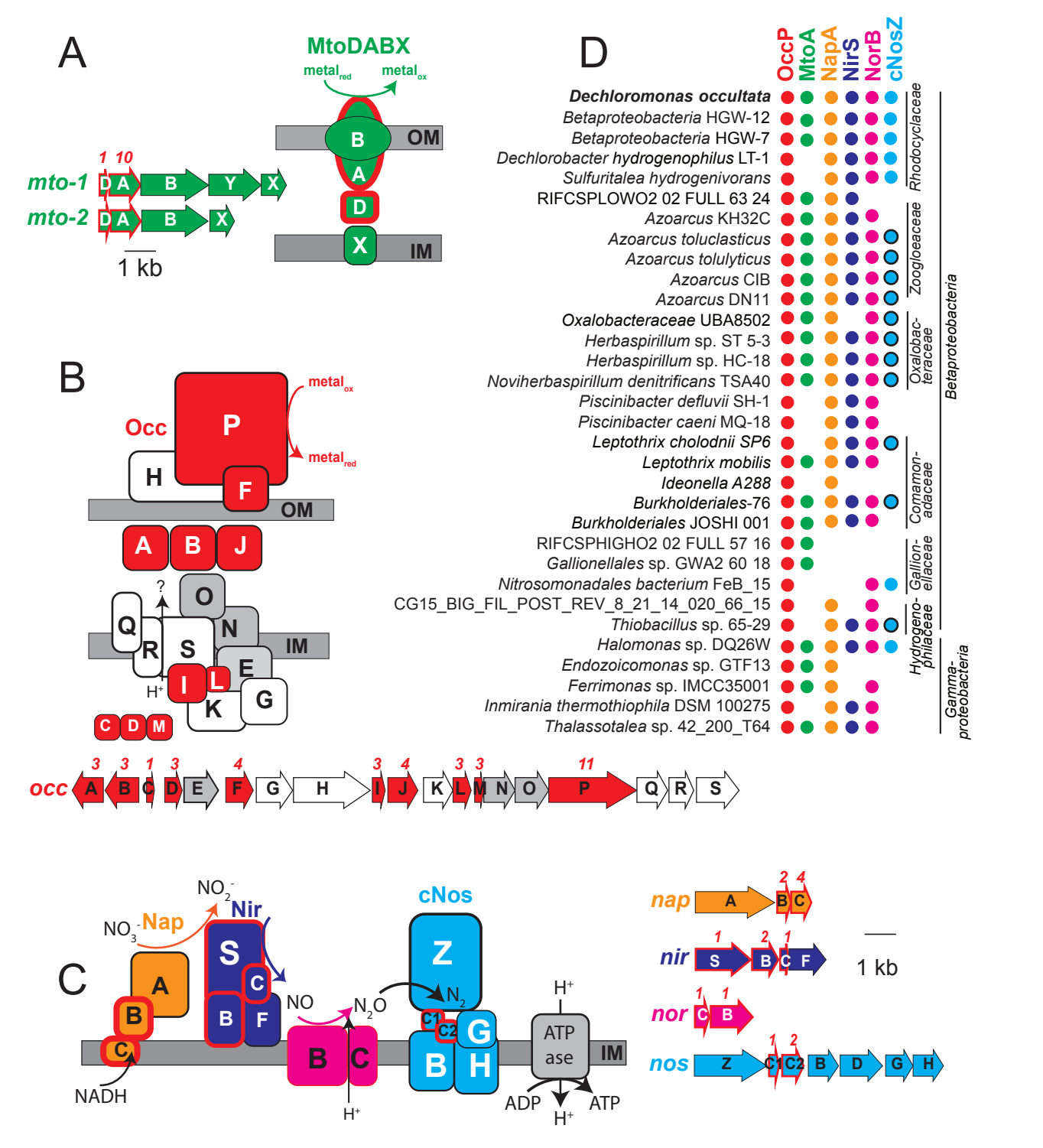
A
MtoDABX
metal_red
metal_ox
B
OM
A
D
X
IM
1 10
mto-1
D A B Y X
mto-2
D A B X
1 kb
B
Occ
P
H
F
OM
metal_ox
metal_red
A B J
?
O
Q
N
R
S
IM
E
I
L
K
G
H+
C D M
occ
3 3 1 3 4
A B C D E F G H
3 4 3 3 11
I J K L M N O P Q R S
D
OccP MtoA NapA NirS NorB cNosZ
Dechloromonas occultata
Betaproteobacteria HGW-12
Betaproteobacteria HGW-7
Dechlorobacter hydrogenophilus LT-1
Sulfuritalea hydrogenivorans
RIFCSPLOWO2 02 FULL 63 24
Azoarcus KH32C
Azoarcus toluclasticus
Azoarcus tolulyticus
Azoarcus CIB
Azoarcus DN11
Oxalobacteraceae UBA8502
Herbaspirillum sp. ST 5-3
Herbaspirillum sp. HC-18
Noviherbaspirillum denitrificans TSA40
Piscinibacter defluvii SH-1
Piscinibacter caeni MQ-18
Leptothrix cholodnii SP6
Leptothrix mobilis
Ideonella A288
Burkholderiales-76
Burkholderiales JOSHI 001
RIFCSPHIGHO2 02 FULL 57 16
Gallionellales sp. GWA2 60 18
Nitrosomonadales bacterium FeB_15
CG15_BIG_FIL_POST_REV_8_21_14_020_66_15
Thiobacillus sp. 65-29
Halomonas sp. DQ26W
Endozoicomonas sp. GTF13
Ferrimonas sp. IMCC35001
Inmirania thermothiophila DSM 100275
Thalassotalea sp. 42_200_T64
Rhodocyclaceae
Zoogloeaceae
Oxalobac-teraceae
Comamon-adaceae
Gallion-ellaceae
Hydrogeno-philaceae
Betaproteobacteria
Gamma-proteobacteria
C
NO3- Nap
NO2- Nir
A
B
C
S
B F
C
NADH
NO
N2O
cNos
Z
C1 C2
G
B H
N2
B C
H+
ATP ase
ADP
ATP
IM
nap A 2 4 B C
nir 1 S 2 B 1 C F
nor 1 1 C B
nos Z 1 2 C1 C2 B D G H
1 kb

bioRxiv preprint doi: https://doi.org/10.1101/695007; this version posted November 1, 2019. The copyright holder for this preprint (which was not certified by peer review) is the author/funder. All rights reserved. No reuse allowed without permission.

Enzyme	Function	SP	TMH	CxxCH	P-sort	NCBI ID	Normalized peptide counts				CH4/N2		P value
							CH_4	SD	N_2	SD	ave	SD	
***Ca.* Dechloromonas occultata**													
Mto-1	MtoX-1 (cyt-b)	N	5	0	IM	RIX49676							
	MtoY-1 (MCP)	N	2	1	IM	RIX49677	2.7	0.5	3.6	0.2	0.8	0.2	0.2
	MtoB-1 (porin)	Y	0	0	OM	RIX49678	10	2	15	2	0.6	0.1	0.004
	MtoA-1	Y	1	10	P	RIX49874	5	1	2.5	0.1	1.9	0.4	0.1
	MtoD-1	N	0	1	P	RIX49875							
Mto-2	MtoX-2 (cyt-b)	N	4	0	IM	RIX48942							
	MtoB-2 (porin)	Y	0	0	OM	RIX48943	8	1	16	0.2	0.5	0.1	0.04
	MtoA-2	Y	1	10	P	RIX48944	7.3	0.8	4	2	2.1	1.3	0.2
	MtoD-2	**Y**	**1**	**1**	**U**	**RIX48945**	**2.6**	**0.3**	**0.7**	**0.3**	**4.0**	**1.4**	**0.003**
Occ	**OccA**	**Y**	**1**	**3**	**P**	**RIX49688**	**4**	**0.5**	**0.7**	**0.6**	**7.8**	**5.7**	**0.01**
	OccB	**Y**	**0**	**3**	**U**	**RIX49689**	**41**	**4**	**19**	**2**	**2.2**	**0.0**	**0.03**
	OccC	N	0	1	U	RIX49877							
	OccD	N	0	3	U	RIX49878							
	OccE (6-NHL)	N	1	0	U	RIX49690	22	2.1	20.5	0.2	1.1	0.1	0.2
	OccF	Y	2	4	E	RIX49691	13	0.7	10.1	0.1	1.3	0.1	0.06
	OccG (PPIase)	**N**	**0**	**0**	**U**	**RIX49692**	**14**	**1**	**3.3**	**0.5**	**4.2**	**0.3**	**0.01**
	OccH	N	0	0	OM/E	RIX49693	6.0	0.2	7.7	0.6	0.8	0.1	0.10
	OccI	N	1	3	U	RIX49694	7	2.5	2.3	0.0	2.9	1.1	0.1
	OccJ	**Y**	**0**	**4**	**U**	**RIX49879**	**44**	**0.2**	**19**	**3**	**2.4**	**0.4**	**0.03**
	OccK	**N**	**0**	**0**	**C**	**RIX49880**	**39**	**6**	**13**	**1**	**3.0**	**0.2**	**0.04**
	OccL	N	1	3	U	RIX49695							
	OccM	N	0	3	U	RIX49881							
	OccN (6 NHL)	N	2	0	U	RIX49696	5.7	0.3	6	1	0.9	0.1	0.2
	OccO (6 NHL)	N	0	0	U	RIX49882	1.2	0.8	4.2	0.4	0.3	0.2	0.03
	OccP	N	0	11	E	RIX49697	14	2	12	3	1.2	0.5	0.4
	OccQ	Y	4	0	IM	RIX49698							
	OccR	N	8	0	IM	RIX49883							
	OccS	N	12	0	IM	RIX49699							
Cyt c	**Cyt c5**	**N**	**1**	**1**	**U**	**RIX47670**	**27**	**2**	**9**	**3**	**3.2**	**0.8**	**0.01**
	Cyt c5	Y	1	2	P	RIX40984	19	2	6	1	**3.3**	**1.0**	0.06
	Cyt c'/C_2	Y	1	1	P	RIX44710	17	5	3.6	0.8	**4.8**	**2.3**	0.09
	Cyt c'/C_2	Y	1	1	P	RIX49630	7	1	1.2	0.9	**8.2**	**6.6**	0.07
	Cyt c551/c552	Y	0	1	P	RIX49087	13	3	2.8	0.0	**4.8**	**1.1**	0.06
	Cyt c4	Y	0	2	P	RIX48804	16	0.8	9.8	0.8	**1.6**	**0.2**	0.06
	Cyt c4	Y	0	2	P	RIX44782	4	2	1.7	0.7	**2.6**	**0.1**	0.08
	Cyt c4	**Y**	**0**	**2**	**P**	**RIX45018**	**7**	**0.6**	**2.2**	**0.2**	**3.0**	**0.0**	**0.02**
Nap	NapA	Y	0	0	P	RIX41011	76	2	67	3	1.1	0.1	0.1
	NapB	**Y**	**1**	**2**	**P**	**RIX41010**	**15**	**1**	**5**	**2**	**3.2**	**0.9**	**0.02**
	NapC	N	1	4	IM	RIX41009	12	3	13	1	1.0	0.2	0.1
Nir	NirS	Y	0	1	P	RIX44719	58	2	44	4	1.3	0.2	0.1
	NirB	Y	1	2	P	RIX44720	14	3	10	2	1.5	0.6	0.2
	NirC	N	0	1	P	RIX44788							
	NirF	Y	1	0	P or C	RIX44721	2	1	7	1	0.3	0.1	0.02
Nor	NorC	N	1	1	IM	RIX45182	3.5	0.7	3.2	0.7	1.1	0.0	0.1
	NorB	N	12	1	IM	RIX45183							
cNos	cNosZ	Y	0	0	P	RIX42539	77	17	66	8	1.2	0.3	0.2
	cNosC1	Y	1	1	P	RIX42538	16	2	4	2	5	3	0.08
	cNosC2	**Y**	**1**	**2**	**P**	**RIX42537**	**10**	**0.1**	**3.9**	**0.3**	**2.6**	**0.1**	**0.02**
	cNosB	N	6	0	IM	RIX42536							
	cNosD	N	0	0	P	RIX42535							
	cNosG	N	1	0	C	RIX42534							
	cNosH	N	4	0	IM	RIX42533							
Qcr	QcrA	N	9	0	CM	RIX41976							
	QcrB	N	9	0	CM	RIX41977							
	QcrC	N	1	0	CM	RIX41978							
Proteases	**Serine protease**	**N**	**0**	**0**	**P**	**RIX49468**	**27**	**2**	**1.0**	**0.3**	**29**	**10**	**0.02**
	Carboxyl-terminal protease (S41)	**N**	**1**	**0**	**CM**	**RIX48818**	**18.5**	**0.8**	**8.0**	**0.9**	**2.3**	**0.1**	**0.0002**
Membrane/Extracellular	**DUF4214 protein**	**N**	**0**	**0**	**OM/E**	**RIX44180**	**146**	**25**	**43**	**0.6**	**3.4**	**0.5**	**0.05**
	S-layer protein	N	0	0	U	RIX44181	8	0.5	10	0.6	0.8	0.1	0.14
	PEP-CTERM sorting	**Y**	**1**	**0**	**E**	**RIX45463**	**68**	**6**	**33**	**10**	**2.1**	**0.5**	**0.03**
	Tol-Pal system protein TolB	**Y**	**0**	**0**	**P**	**RIX44015**	**20**	**2**	**12**	**1**	**1.67**	**0.05**	**0.03**
	Peptidoglycan-associated lipoprotein (Pal)	**N**	**0**	**0**	**OM**	**RIX44016**	**27.3**	**0.2**	**10**	**3**	**3**	**1**	**0.04**
	Tol-Pal system protein YbgF	Y	0	0	U	RIX44017	10.8	0.4	4	2	4	2	0.06
	Pilus assembly protein	**N**	**0**	**0**	**U**	**RIX46961**	**54**	**5**	**30**	**5**	**1.8**	**0.1**	**0.001**
Other	**PQQ-dependent dehydrogenase**	**Y**	**0**	**0**	**P**	**RIX45050**	**37**	**4**	**17**	**1**	**2.2**	**0.1**	**0.03**
	Phasin family granule-associated protein	**N**	**0**	**0**	**U**	**RIX40682**	**49**	**2**	**22**	**1**	**2.2**	**0.2**	**0.03**
	Phasin family granule-associated protein	**Y**	**0**	**0**	**U**	**RIX40683**	**34**	**4**	**16**	**1**	**2.1**	**0.0**	**0.03**
	High potential iron-sulfur protein	**Y**	**0**	**0**	**U**	**RIX49681**	**10.79**	**0.01**	**6.5**	**0.4**	**1.7**	**0.1**	**0.02**
	Electron transfer flavoprotein (FixA)	**N**	**0**	**0**	**C**	**RIX43544**	**16**	**3**	**10**	**2**	**1.7**	**0.0**	**0.04**
***Ca.* Geobacter occultata**													
E-pilus	**Type IV pilin PilA**	**N**	**1**	**0**	**E**	**RNC67631**	**93**	**3**	**18**	**3**	**5**	**1**	**0.02**